IVYSPRING INTERNATIONAL PUBLISHER

Theranostics

2012; 2(7):705-713. doi: 10.7150/thno.3456

Research Paper

Bioconjugated Pluronic Triblock-Copolymer Micelle-Encapsulated Quantum Dots for Targeted Imaging of Cancer: In Vitro and In Vivo Studies

Liwei Liu[1,2] ✉, Ken-Tye Yong[3] ✉, Indrajit Roy[4], Wing-Cheung Law[2], Ling Ye[5], Jianwei Liu[5], Jing Liu[5], Rajiv Kumar[2], Xihe Zhang[1], Paras N. Prasad[1,2]

1. School of Science, Changchun University of Science and Technology, Changchun 130022, Jilin, China.
2. Institute for Lasers, Photonics and Biophotonics (ILPB), The State University of New York at Buffalo, Buffalo, NY14260, United States.
3. School of Electrical and Electronic Engineering, Nanyang Technological University, 639798, Singapore.
4. Department of Chemistry, University of Delhi, Delhi, 110007, India.
5. Institute of Gerontology and Geriatrics, Chinese PLA General Hospital, Beijing 100853, China.

✉ Corresponding author: Dr. Ken-Tye Yong, School of Electrical & Electronic Engineering, Nanyang Technological University, 639798, Singapore. Email: ktyong@ntu.edu.sg, Dr. Liwei Liu, School of Science Changchun University of Science and Technology Changchun, P.R.China 130022. Email: liulw@cust.edu.cn.

Received: 2011.08.28; Accepted: 2011.10.19; Published: 2012.07.28

Abstract

Early in this study, CdTe/ZnS core/shell quantum dots (QDs) were encapsulated in carboxylated Pluronic F127 triblock polymeric micelle, to preserve the optical and colloidal stability of QDs in biological fluids. Folic acid (FA) was then conjugated to the surface of QDs for the targeted delivery of the QD formulation to the tumor site, by exploiting the overexpressed FA receptors (FARs) on the tumor cells. Cytotoxicity study demonstrated that the QD formulation has negligible *in vitro* toxicity. The *in vitro* study showed that the bioconjugated micelle-encapsulated QDs, but not the unconjugated QDs, were able to efficiently label Panc-1 cancer cells. *In vivo* imaging study showed that bioconjugated QDs were able to target tumor site after intravenous injection of the formulation in tumor-bearing mice.

Key words: Quantum dots, Targeted delivery, Bioimaging, Bioconjugation, Pluronics and Nanotoxicity.

Introduction

Nanotechnology has received a great deal of attention in the fields ranging from biology to medicine [1-6]. Quantum dots (QDs) are known to be a potential candidate as optical probes for long term imaging *in vitro* and *in vivo* due to their unique optical properties, such as bright fluorescence, narrow emission, broad excitation, and high photostability [7-11]. In general, the fabrication of QDs is commonly carried out in organic solvents at high temperature to produce high-quality nanocrystals. However, the prepared QDs are not water dispersible. In order to employ QDs for biosensing and biomedical imaging applications, they need to be water-dispersible and biocompatible with the biological environment [12-15]. An alternative approach is to prepare QDs in aqueous phase and excellent stability was shown in the prepared QD [16-17]. There are also many reports in the literature reporting on the surface modification of QDs; for example, by functionalizing small molecules such as mercaptoacetic acid to QDs surface, coating silica layer around the QDs, and encapsulating QDs within liposomes and amphiphilic polymer nanopar-

ticles [18-21]. However, some of the mentioned approaches above displayed some disadvantages such as requiring complicated steps and long hours of preparation, and the intrinsic instability of the formulation that will lead to the breakdown QDs in solution [22, 23]. Furthermore, some of these methods have led to the broadening of emission spectra and severe quenching of the emission intensity.

The amphiphilic triblock copolymer, Pluronic, consisting of poly(ethylene oxide) (PEO) and poly(propylene oxide) (PPO) blocks with a PEO–PPO–PEO structure, have been studied for the last ten years in applications ranging from drug to gene carriers [24-32]. Pluronic exists in various compositions and they can self-assemble into polymeric micelles with various morphologies depending on the aqueous solvent quality, the critical micelle concentration (CMC), and critical micelle temperature (CMT). The triblock copolymer micelles are composed of a hydrophobic core that serves as a cavity for the encapsulation of hydrophobic agents, and a hydrophilic shell that provides aqueous stability [33-38]. Therefore, the micelles can be used to load high concentration of drugs for cancer therapy. In addition, these micelles have metabolic stability and long circulation time in blood. Pluronic F127 triblock-copolymer micelle nanoparticles are considered as one of the most studied biocompatible polymer nanocarriers for *in vivo* studies [39,40]. These Pluronic F127 micelle particles meet all the requirements for therapeutic and biomedical applications *in vitro* and *in vivo*, such as biocompatibility, biodegradability, low toxicity, and the ability to encapsulate high dosage of drugs and to cross some biological barriers [41]. For example, doxorubicin molecules encapsulated in Pluronic F127 micelles have been successfully evaluated in Phase II study in patients with advanced esophageal carcinoma. Moreover, the micellar size is less than 120 nm, which makes them suitable for prolonged circulation in blood and easy extravasation to tumor tissues *in vivo* [42].

Folic acid (FA) is generally taken up into the cells by the folate receptor (FAR). When FA binds to FAR on the surface of tumor cells, this process will initiate the receptor-mediated endocytosis [43]. For tumor growth in body, high level of nucleic acid synthesis is required to meet the demands of proliferating cells. Thus, elevated quantities of FA are needed for this process. FAR is overexpressed in many human cancer tumors. For example, it is reported to be overexpressed in human nasopharyngeal carcinoma (KB) cells, and several other established cancer cell lines such as cancer cells originating from ovary, cervix, pancreas, breast, and myeloid leukemia [44]. Our group has previously demonstrated the use of FA conjugated QDs as highly biocompatible probes for two photon imaging of cancer cells [45]. Though FA has been used as targeting molecules in many *in vitro* imaging studies, there are limited reports available using FA conjugated QDs for targeted *in vivo* cancer imaging. Thus, it is important for us to understand the tumor-specificity of the FA-conjugated QDs and their in vivo biodistribution for targeted cancer imaging. These findings will be served as important guidelines for us to optimize the formulation for clinical research purpose.

In this study, highly luminescent CdTe/ZnS core/shell QDs were synthesized and were encapsulated within the Pluronic F127 micelle nanoparticles for *in vitro* and *in vivo* bioimaging applications. More specifically, Pluronic F127 micelles were used to enable stable dispersion of QDs in biological fluids, generating a hydrophilic shell with PEG molecules on its surface. In addition, the carboxyl groups are terminated on their surface for bioconjugation purpose. For *in vitro* studies, these encapsulated QDs were conjugated with FA and used as luminescent probes for cancer cell imaging studies. The *in vivo* tumor targeting and imaging study of FA conjugated micelle-encapsulated QDs was evaluated by using whole-body small animal optical imaging system. Our studies have shown high reproducibility in tumor targeting of the bioconjugated micelle-encapsulated QDs *in vivo*, following systemic administration. The formulation demonstrated low toxicity to the treated mice. This information provides an important platform in creating the next generation of multifunctional probes for targeted cancer imaging.

Materials and Methods

Materials

Pluronic® F127 (F127) was kindly provided by BASF (Butte, MT, USA). Folic acid, maleic anhydride, toluene, pyridine, diethyl ether, HPLC water and N-(3-Dimethylaminopropyl)-N′-ethylcarbodiimide hydrochloride (EDC), 3-Mercaptopropionic acid (MPA), tellurium (Te) powder, cadmium chloride ($CdCl_2$), zinc acetate, dodecanethiol, trioctylphosphine (TOP), trioctylphosphine oxide (TOPO), sodium borohydride ($NaBH_4$) and sulfur (S) were used as received from Sigma-Aldrich (St. Louis, USA). The tetrazolium compound [3-(4, 5-dimethylthiazol-2-yl)-5-(3-carboxymethoxy-phenyl) -2-(4-sulophenyl)-2H-tetrazolium, inner salt; MTS] was purchased from Promega (WI, USA). All other chemicals were obtained from Sigma-Aldrich (St. Louis, USA).

Synthesis and characterization of carboxylated Pluronic F127 ABA triblock copolymer

The carboxylated ABA triblock copolymer F127 (F127COOH) can be obtained according to the reported work, as shown in Figure 1 [46, 47]. The ^{1}H-NMR spectrum recorded on INOVA-500 spectrometer confirmed the formation of chemical structure of F127-COOH using deuterium chloroform (d-$CDCl_3$) as a solvent with tetramethylsilane (TMS) as an internal standard.

Synthesis of CdTe/ZnS core/shell QDs

Synthesis of CdTe/ZnS QD was based on the procedures reported previously [11]. Briefly, 128 mg of tellurium powder and 80 mg of sodium borohydride were mixed with 5 mL of degassed water. The mixture was stirred for 2-3 h until a light-pink solution was observed. We refer this solution as the Te precursor. Next, 2 mmol of $CdCl_2$, 5 mmol of MPA, and 150 mL of water were mixed into a three-necked flask under stirring. The pH was adjusted to 8.5 by adding sodium hydroxide solution. The flask was sealed and 1.5 mL of Te precursor was injected quickly into the mixture under nitrogen. The reaction mixture was slowly heated to 100 °C. At the desired emission wavelength, the QDs were purified from the surfactant solution by adding ethanol and centrifugation. The QDs synthesized in aqueous solution were transferred to organic phase using dodecanethiol according to a reported protocol with slight modifications [48, 49]. Briefly, purified QDs were dispersed into 5 mL of water and then a mixture of 5 mL of dodecanethiol, 5 mL of butanol and 2 mL of acetone was added. After stirring for 2 min, 200 µL of NH_4OH was added. The transferred QDs were purified and re-dispersed in chloroform by the addition of ethanol and centrifugation. For ZnS shell coating, a solution containing 5 g of trioctylphosphine oxide, 5 mL of oleic acid and 2 mmol of zinc acetate were prepared and heated to 100 ^oC under nitrogen until a clear solution was observed. The CdTe core solution was injected slowly under stirring into the hot reaction mixture with a needle outlet that allowed chloroform to evaporate. The temperature was then raised to 170-180 ^oC. Upon reaching the desired temperature, 1 mL of 1 mM TOP-S solution (32 mg of sulfur dissolved in 1 mL of TOP) was added dropwise into the reaction mixture. The mixture was then maintained at ~180 ^oC for 2-5 min and then separated by addition of ethanol and centrifugation.

Preparation of FA conjugated micelle-encapsulated QDs

In this preparation, hydrophobic QDs (~3.0 mg) were mixed with F127COOH (~20 mg) in chloroform. The organic solvent was evaporated off under vacuum and the deposited film on the vials was hydrated with 1.0 mL of HPLC water. The obtained aqueous dispersion of nanoparticle was filtered through 0.2 µm membrane filter and kept at room temperature for further bioconjugation. The 1.0 mL of F127COOH-QDs aqueous solution obtained from previous step was activated by 100 µL of EDC solution (9.6 mg/mL in water; 5.2 x 10^{-6} mol) for 5-10 min and 80 µL of FA solution in DMSO (~14 mg/mL, 4.67x10^{-10} mol) was added. After 1.5 h of conjugation, the pellets of FA conjugated F127COOH-QDs (FA-F127COOH-QDs) NPs were collected by centrifugation under 13,000 rpm for 15 min, and then re-dispersed in ~400 µL of sterile water for further applications.

Characterization of micelle-encapsulated QDs

The UV/vis absorbance and the PL were acquired at room temperature using a Shimadzu UV-3600 spectrophotometer and a Fluorolog-3 spectro-fluorometer (Jobin Yvon, Longjumeau, France) over a wavelength range from 300 to 800 nm with light source: 420 nm, integration time: 100 ms and PMT voltage: 1 kV, respectively. The samples were measured against water as reference. All samples were used as prepared and loaded into a quartz cell for measurements. Quantum yields (QY) were obtained by comparing the integrated emission value of the QDs to a standard dye, Rhodamine 6G (QY = 0.95) in ethanol. The sample absorbance was matched to 0.030 ± 0.003 at the excitation wavelength of 480 nm. Transmission electron microscopy (TEM) images were obtained using a JEOL model JEM-100CX microscope at an acceleration voltage of 80 kV to determine the size and shape of the prepared QD formulation. The specimens were prepared by drop casting the sample dispersion onto an amorphous carbon coated 300 mesh copper grid, which was placed on a filter paper to absorb the excess solvent. A 90Plus Particle Size Analyzer (Brookhaven Instruments Corporation, USA) was used to measure the hydrodynamic size and the zeta potential values of the nanoparticles.

In vitro cytotoxicity studies

The Panc-1 cells were selected and cultured in 96-well tissue microtiter plate using the DMEM medium plus 10% FBS, until reaching ~5×10^3 cells per well. The MTS assay was carried out according to the manufacturer's instructions (Promega). Colorimetric measurements were performed at 490 nm with a scanning multi-well spectrometer using Opsys MR

Autoreader system (Opsys MR Autoreader, Dynex Technologies Inc., Chantlly, VA, USA). The Absorbance values for untreated wells were taken as control reference (100% survival). In brief, after 24 and 48 h hours treatment with the FA-F127COOH-QD nanoparticles (from 1-5 mg/mL), media was rinsed and 15 µL of MTS reagent was added to each well and well-mixed. The absorbance of the mixtures at 490 nm was measured after incubating for 2-3 h at 37 °C in cell culture incubator. Tests were performed in triplicate. Each point represents the mean ± SD (bars) of replicates from one representative experiment.

Cell staining studies with bioconjugated QD formulation

Panc-1 cells were seeded in 35 mm LabTek plates prior to experiment. Confocal Laser Scanning Microscopy (CLSM) was applied to obtain confocal imaging using a Leica TCS SP2 AOBS spectral confocal microscope (Leica Microsystems Semiconductor GmbH, Wetzler, Germany) with laser excitation at 488 nm and emission between 530-730 nm with x64 microscope object lens (UPlan Olympus). All images were taken under exact same conditions of laser power, aperture, gain, offset, scanning speed, and scanning area.

Targeted tumor imaging studies using bioconjugated micelle-encapsulated QDs

In vivo optical imaging of the Panc-1 tumor bearing mice body were evaluated by non-invasive optical imaging technology using a Maestro GNIR FLEX fluorescence imaging system (Cambridge Research & Instrumentation, CRI; Model: M-MS1-500-Flex). Female athymic nude mice were used, with subcutaneously xenografted Panc-1 tumors on their shoulder. In these tumor-bearing mice, 200 µL of the prepared FA-F127COOH-QDs in sterile water was injected via tail vein. Animal experiments were performed in compliance with guidelines set by the University at Buffalo. Imaging was done immediately after the injection. Excitation was done at 455-490 nm by the xenon lamp. The emission filter of 515 nm longpass was used to cut off excitation light. Wavelength-resolved spectral imaging was carried out using a spectral imaging system (CRI) comprising an optical head that includes a liquid crystal tunable filter, an optical coupler, and a scientific-grade monochrome CCD camera, along with image acquisition and analysis software (Nuance 1.4.2). The tunable filter was automatically stepped in 10 nm increments from 515 to 950 nm, while the camera captured images at each wavelength with constant exposure. The overall acquisition time was about 12 s. The resulting TIFF images were loaded into a single data structure in the memory, forming a spectral stack with a spectrum at every pixel. With spectral imaging software, small but meaningful spectral differences could be rapidly detected and analyzed. The autofluorescence spectra and the FA-F127COOH-QD spectra were manually selected from the spectral image to select appropriate regions. Spectral unmixing algorithms were applied to create the unmixed images of "pure" autofluorescence and "pure" QD signal. When appropriately generated, the autofluorescence image should be uniform in intensity, regardless of the presence or absence of the QD signal. The identification of valid spectra for unmixing purposes need only be done initially, as the spectra can be saved in spectral libraries and reused on additional spectral stacks.

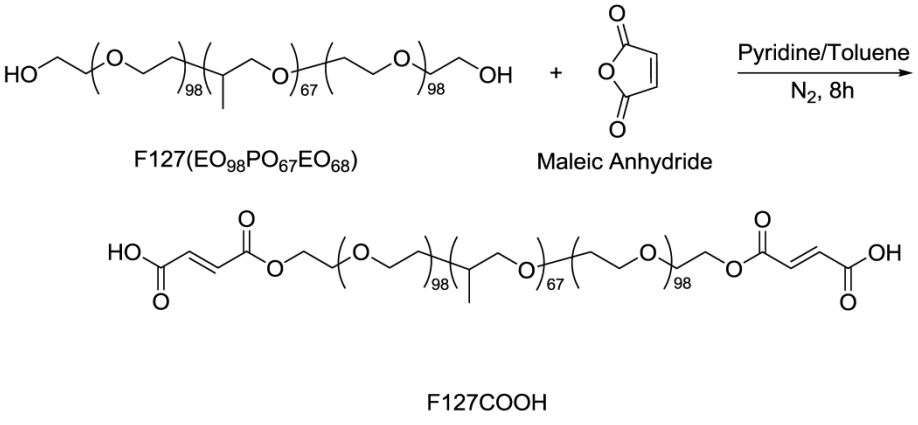

Figure 1. The illustration of synthetic route of carboxylated triblock copolymer F127 (F127COOH).

Results and Discussion

Figure 1 illustrates the synthesis of carboxyl terminated Pluronic F127 triblock polymer. The obtained ^{1}H-NMR spectra confirmed that we have successfully transformed Pluronic F127 to F127COOH. In the spectrum of F127, chemical shifts (δ) were observed at 1.1 (m), 2.0 (s), 3.3 (m), 3.4 (m), 3.5 (m) ppm, which belong to the hydrogen atoms of -CH-CH_3, -CH_2-O-H, -CH-CH_3, -CH-CH_2-O-, and –O-CH_2-CH_2-O- groups, respectively. After the carboxyl groups were introduced onto the PEO structure (the structure of F127COOH), the signal of δ = 4.3 ppm (=CH-COOH) emerged while the δ = 2.0 ppm signal coming from protons of –CH_2-OH disappeared. More importantly, two resonance peaks at δ = 6.3 (m) and 6.5 (m) ppm of the ethylene linkage in the structure of F127COOH, which came from the regimen of maleic acid, confirmed successful introduction of carboxyl groups into F127 copolymer chain segments. The synthetic yield of F127COOH from F127 was estimated to be 85% by acid-based titration.

FA conjugation with the carboxyl groups terminated micelle-encapsulated QDs were carried out through EDC chemistry (see Figure 2). In the process of conjugation, we found that concentration between micelle-encapsulated QDs and FA (0.1 and 0.01 μM for QDs and activated FA, respectively) plays an important factor in producing non-aggregating bioconjugated QDs. TEM images of the QDs showed that, after conjugation with a suitable amount of FA, the QDs remained monodispersed and maintained their optical and colloidal properties for more than six months.

For the structure of micelle-encapsulated QDs, QDs are coated in sequence of coordinating ligands, such as hydrophobic surfactants (TOPO and oleic acid), the hydrophobic section of triblock polymer (PPO-$(PEO)_n$-COOH) and hydrophilic section of triblock polymer (PPO-$(PEO)_n$-COOH). The oil-like layer between TOPO/oleic acid with PPO formed a lamellar layer to protect the inner QDs. Meanwhile, the carboxyl group on the PEO surface plays an important role for QDs to maintain the colloidal stability, as well as to provide site for the biomolecule conjugation with the purpose of cell targeting. The micelle-encapsulated QD samples, with or without FA conjugation, can remain well-suspended in aqueous dispersion under pH 7.4, with no aggregation for more than six months at ambient temperature and no loss of any photoluminescence intensity.

Figure 3 shows the UV-visible absorbance and photoluminescence (PL) spectra from the mono-dispersed micelle-encapsulated QD solution (F127-QD). The PL spectrum of the micelle-encapsulated QDs showed a band-edge emission around 700 nm. The quantum yield (QY) of the QDs dispersed in buffer was estimated to be about 45%. No quenching was observed throughout the preparation of the encapsulation process. It is worth mentioning that there was a ~25 nm red shift of emission peak after the encapsulation which can be accounted for the change in the dielectric constant of the medium surrounding the QDs. After the encapsulation, the QD were well protected from the outside environment and thus the emission was not affected by the FA conjugation (see Figure 3). Figure 4a shows the TEM image of the organically dispersible CdTe/ZnS QDs, where their sizes were estimated to be 4.5 nm. Figure 4b shows the TEM image of micelle-encapsulated QDs and their size distribution was determined to be 79.8 ± 14.3 nm. The larger clumps as shown in Figure 3b are interpreted as micelle aggregates. The morphology of the micelle-encapsulated QDs is mostly spherical and no aggregation and precipitation is observed upon storage in the refrigerator.

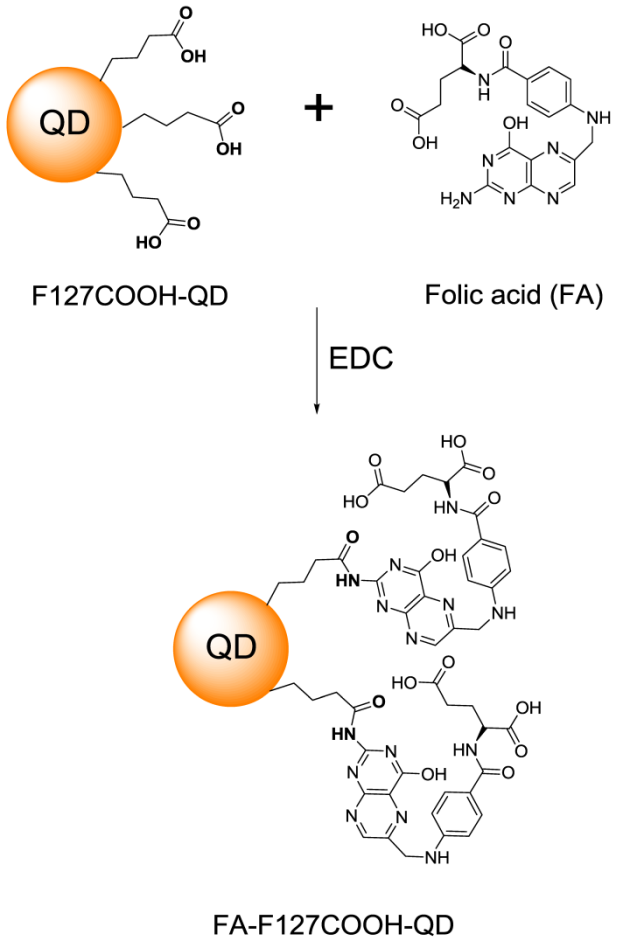

Figure 2. The illustration of conjugation of FA to the micelle-encapsulated QDs.

In addition to TEM study, DLS was used to determine the hydrodynamic size distribution and colloidal stability of the micelle-encapsulated QD dispersion in PBS buffer. As shown in Figure 5a and 5b, the average hydrodynamic size of micelle-encapsulated QDs was determined to be 104.6 ± 3.6 nm (PDI = 0.046) and which was increased to 114.1 ± 4.7 nm upon conjugatiion with FA. Both DLS and TEM result showed good agreement in providing the size of micelle-encapsulated QDs. The zeta potential of micelle-encapsulated-QDs was also measured. The zeta potential was determined to be −32.5 ± 3.0 mV for the QD formulation indicating the presence of carboxyl groups on the outer shell of the micelle-encapsulated QDs. Upon conjugating the QDs with FAs, the surface charge changed to -18.7 ± 2.2 mV. It is worth noting that a zeta potential of -8.2 ±2.1 mV was determined for the micelle-encapsulated QDs in PBS buffer using unmodified Pluronic F127 (without the addition of carboxyl groups).

Prior to embarking on *in vitro* and *in vivo* studies, the cytotoxicity of the micelle-encapsulated QDs was evaluated by MTS cell viability assay, using the Panc-1 cell line. From our findings, we have observed that the cell viability of Panc-1 cells was maintained above 80% with concentration as high as 5.0 mg/mL, at 24 and 48 h post-treatment (Figure 6). The cytotoxicity data suggests that the prepared Pluronic micelle-encapsulated QD formulation have negligible *in vitro* toxicity and demonstrate their usefulness for long term *in vitro* and *in vivo* imaging studies.

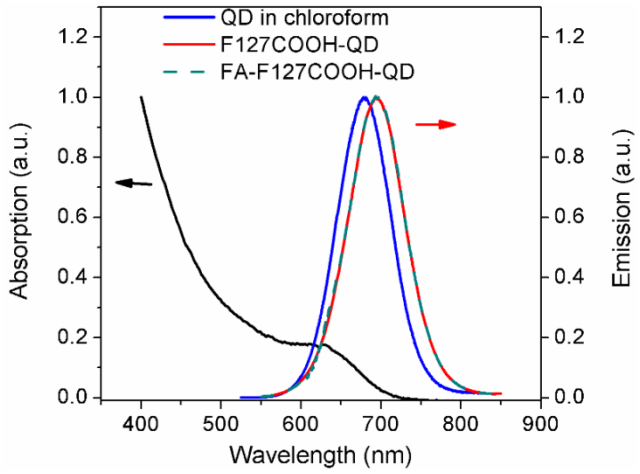

Figure 3. UV-vis absorption (black) and PL (red) spectra of monodispersed Pluronic micelle-encapsulated QDs solution.

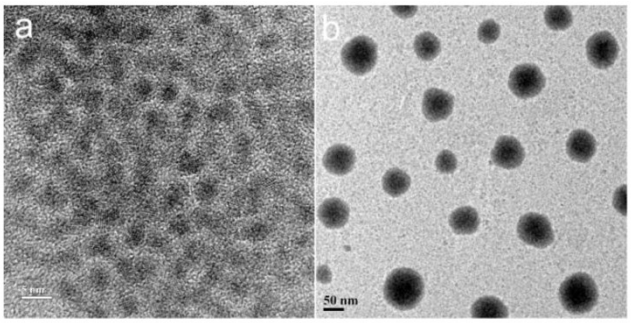

Figure 4. TEM images CdTe/ZnS QDs dispersed in organic media (a) and aqueous media (b). The scale bars are 5 nm and 50 nm, respectively for a) and b).

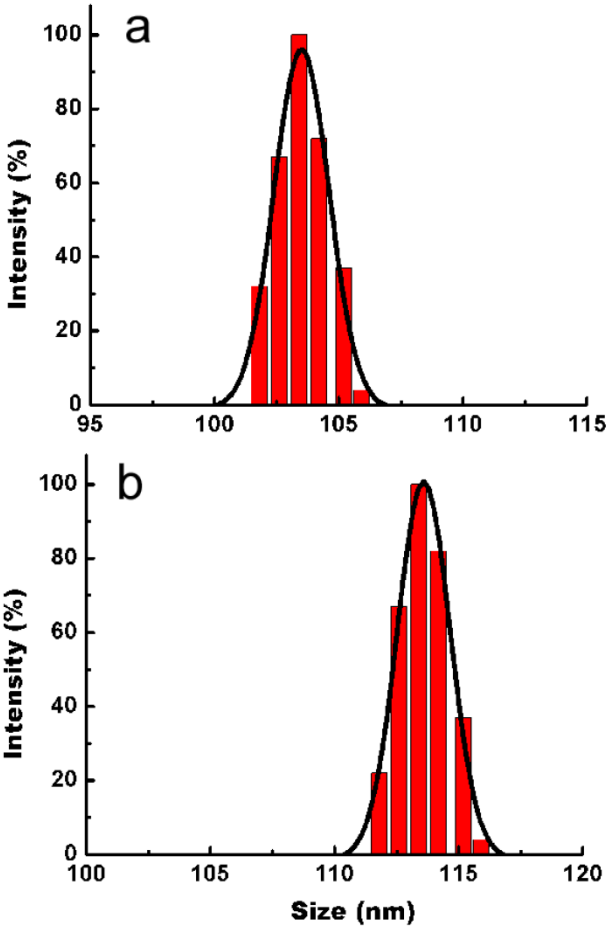

Figure 5. DLS plots of micelle-encapsulated QDs before (a) and after (b) conjugating with FA.

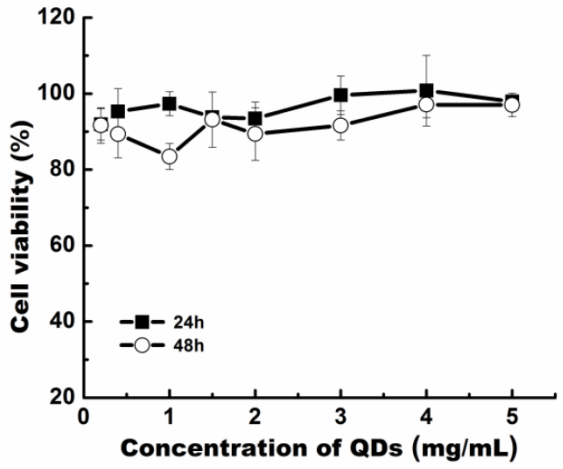

Figure 6. Relative cell viability of Panc-1 cells treated with bioconjugated QD formulation for 24 and 48 h post-treatment.

For *in vitro* studies, confocal microscopy was used to evaluate the uptake of FA-conjugated QDs in Panc-1 cells. As shown in Figure 7, the Panc-1 cells were stained with the bioconjugated QDs after incubating them with QD formulation for 2 h, and no uptake of QDs were observed from the cells when unconjugated micelle-encapsulated QDs were used (see Figures 7a and 7b). In addition to the experiments mentioned above, we have performed an additional experiment to confirm that the uptake of bioconjugated QDs is mediated by the interaction between FA and FAR. The experiment involved saturating the cells with free FA molecules for 2 h in order to block the available FARs on the cell surface, followed by treatment with bioconjugated QDs. In this case, minimal signal from the cells was observed (see Figure 7c), confirming that the bioconjugated micelle-encapsulated QD uptake occurred predominantly *via* the specific interaction between FAs and FARs.

To demonstrate the use of FA conjugated micelle-encapsulated QDs for targeted tumor imaging, the bioconjugated QDs (~4 mg) was administered in tumor-bearing mice by intravenous injection. After 10 min, the mice were anesthetized for whole body luminescence imaging. The Maestro imaging system was used to capture the luminescence images of the treated animals. Figure 8 shows the luminescence images of tumor-bearing mice treated with bioconjugated and non-bioconjugated QDs. As shown in Figure 8, intense QD signals can be detected from the tumor of the mouse intravenously injected with bioconjugated QDs. Also, we can determine that the QD signal (red) can be separated from the autofluorescence background (green). On the other hand, little QD signal was detected from the tumor area of the mouse injected with non-bioconjugated QDs, thus indicating that the tumor-specificity of the FA conjugated micelle-encapsulated QDs. It is worth mentioning that the QD signal can be observed from the tumor as early as 10 min post-injection, although maximum uptake of QDs in the tumor matrix was achieved at 20 min post-injection. We have also observed that the QD signal was detected from other body parts of the mice treated with both bioconjugated and non-bioconjugated QDs, which is due to a result of non-specific systemic distribution of the QDs.

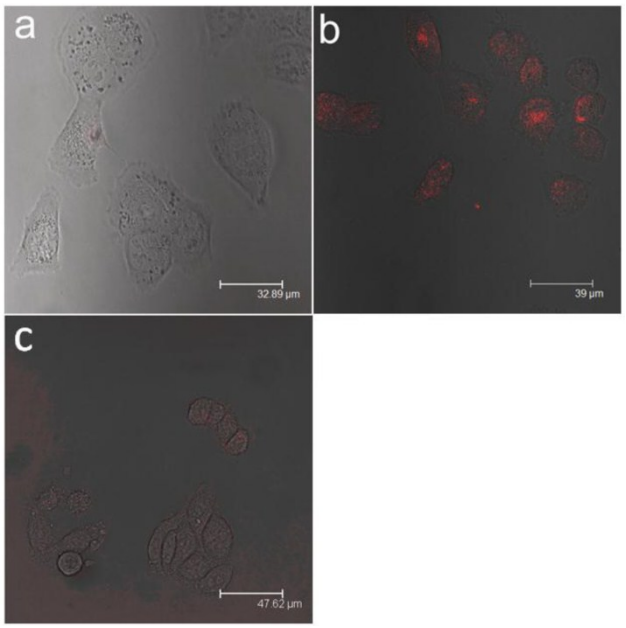

Figure 7. Confocal microscopic images of Panc-1 cells treated with (a) unconjugated micelle-encapsulated QDs (b) FA conjugated micelle-encapsulated QDs and (c) FA conjugated micelle-encapsulated QDs with pre-saturation. In both cases, red represents emission from CdTe/ZnS QDs.

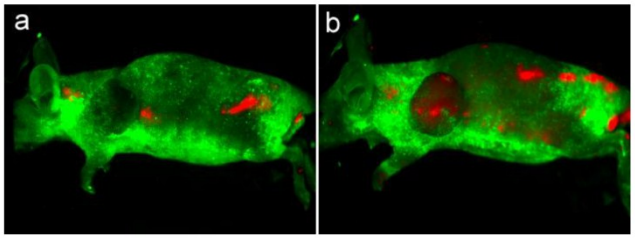

Figure 8. *In vivo* luminescence imaging of Panc-1 tumor-bearing mice injected with non-bioconjugated QDs (a) and ~4 mg of FA conjugated QDs (b), respectively. All images were acquired under the same experimental conditions. The autofluorescence from mice is coded green and the unmixed QD signal is coded red.

To investigate the biodistribution of FA conjugated micelle encapsulated QDs in the tumor-bearing mice, the mice were sacrificed and major organs and tumor were removed for luminescence imaging after intravenously injected with 4 mg of QDs bioconjugates for 3 to 4 h. Figure 9 shows luminescent images of heart, liver, spleen, lung, and kidney obtained from a mouse after injection of FA-QD formulation. As observed from the characteristic red-emitting color of QDs, the QDs are mainly accumulated in the tumor, with some QDs accumulation in the liver, spleen, and kidney. No accumulation of QDs was observed in the heart and lung. Previously, Gao et al. reported the use of functional CdSe/ZnS QDs for in vivo tumor imaging by incorporating QDs into the core of block copolymer nanoparticles [12]. They have reported a similar trend of QD biodistribution in the organs.

In addition to *in vitro* and *in vivo* imaging studies, histological analysis was performed on the tissues obtained from the major organs such as liver, spleen, and kidney post-mortem to investigate signs of acute toxicity. Tissues were harvested one week after intravenous injection the micelle-encapsulated QDs BALB/c mice. As shown in Figure 10, no signs of toxicity were observed from the animals receiving the QDs at concentration as high as 160 mg/kg as compared to the H&E-stained tissue sections from the animal treated with PBS buffer solution [9].

In this study, we have demonstrated the synthesis of FA conjugated micelle-encapsulated QDs, which can be used for targeted tumor imaging *in vitro* and *in vivo*. We envision that the carboxyl groups terminated micelle-encapsulated QD formulation can serve as a useful platform for conjugation with various biomolecules such as antibodies and peptides, for targeted *in vivo* delivery. Also, the micelle-encapsulated QDs can be further incorporated with additional contrast reagents and therapeutic drugs for multimodal imaging and traceable targeted drug delivery applications. More importantly, Pluronic micelles have been used as a FDA approved drug delivery system for the last decade and it was reported that Pluronic copolymers can reduce multidrug resistance to anti-cancer agents through the internalization mechanism of the drug and reducing its efflux from cells mediated by P-glycoprotein. Thus, the Pluronic micelle-encapsulated QDs system reported in this study have the potential to be translated for clinical research for image-guided therapy, where they can overcome multidrug resistance in tumors and thus markedly increase therapeutic efficiency.

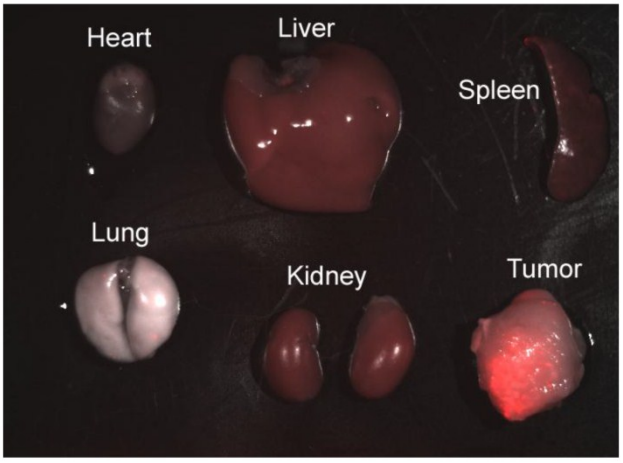

Figure 9. Luminescent image of resected organs from Panc-1 tumor-bearing mouse injected with FA-conjugated micelle-encapsulated QDs. The luminescent image shows the overlays of florescence and transmission images.

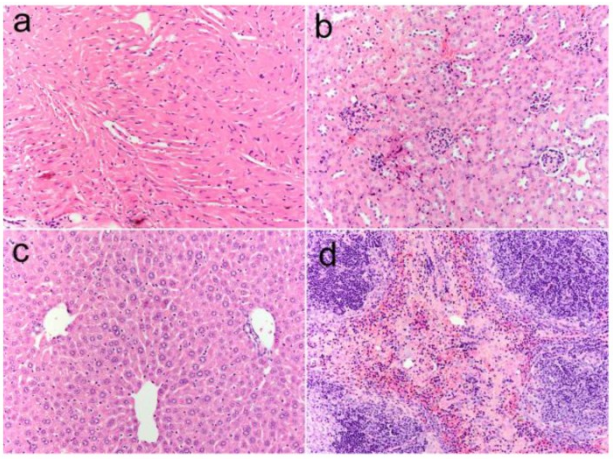

Figure 10. H&E-stained tissue sections from mice administered with micelle-encapsulated QDs two weeks post injection. Tissues were harvested from heart (a), kidney (b), liver (c), and spleen (d).

Conclusion

In summary, we report a simple method of synthesis of Pluronic micelle-encapsulated QDs as nanoprobes for cancer imaging. Our design was not only able to protect the QDs stable enough under physiological conditions but also can be conjugated with FA by the simple EDC chemistry conjugation technique, for targeted cancer imaging applications. The result of preliminary work with this nanoprobe appeared to be promising, which revealed the potential of this nanoprobe for *in vivo* application due to the negligible level of toxicity. We have confirmed the targeting of QD bioconjugates in a pancreatic tumor model using small animal imaging system.

Conflict of Interest

The authors have declared that no conflict of interest exists.

Acknowledgments

This study was supported by grants from the John R. Oishei and in part by the Singapore Ministry of Education under Research Grant MOE2010-T2-2-010.

References

1. Bhirde A, Guo N, Chen XY. Targeted nanoprobes reveal early time point kinetics in vivo by time-resolved MRI. Theranostics. 2011;1:274-276.
2. Prasad PN. Nanophotonics. New York: Wiley-Interscience. 2004.
3. Prasad PN. Introduction to Biophotonics. New York: Wiley-Interscience. 2004.
4. Kairdolf BA, Smith AM, Nie S. One-Pot Synthesis, Encapsulation, and solubilization of size-tuned quantum dots with amphiphilic multidentate ligands. J Am Chem Soc. 2008; 130: 12866-7.
5. Kiessling F, Gaetjens J, Palmowski M. Application of molecular ultrasound for imaging integrin expression. Theranostics. 2011;1:127-134.
6. Zhang F, Zhu L, Liu G, Hida N, Lu GM, Eden HS, et al. Multimodality Imaging of Tumor Response to Doxil. Theranostics. 2011;1:302-309.
7. Anikeeva PO, Halpert JE, Bawendi MG, Bulovic V. Quantum dot light-emitting devices with electroluminescence tunable over the entire visible spectrum. Nano Lett. 2009;9:2532-6.
8. Bharali DJ, Lucey DW, Jayakumar H, Pudavar HE, Prasad PN. Folate-receptor-mediated delivery of InP quantum dots for bioimaging using confocal and two-photon microscopy. J Am Chem Soc. 2005; 127: 11364-71.
9. Susumu K, Uyeda HT, Medintz IL, Pons T, Delehanty JB, Mattoussi H,et al. Enhancing the stability and biological functionalities of quantum dots via compact multifunctional ligands. J Am Chem Soc. 2007; 129: 13987-96.
10. Yong K-T, Roy I, Hu R, Ding H, Cai H, Zhu J, et al. Synthesis of ternary CuInS2/ZnS quantum dot bioconjugates and their applications for targeted cancer bioimaging. Integr Biol. 2009; 2: 121-9.
11. Law W-C, Yong K-T, Roy I, Ding H, Hu R, Zhao W, et al. Aqueous-phase synthesis of highly luminescent CdTe/ZnTe core/shell quantum dots optimized for targeted bioimaging. Small. 2009; 5: 1302-10.
12. Gao X, Cui Y, Levenson RM, Chung LWK, Nie S. In vivo cancer targeting and imaging with semiconductor quantum dots. Nat Biotechnol. 2004; 22: 969-76.
13. Jamieson T, Bakhshi R, Petrova D, Pocock R, Imani M, Seifalian AM,et al. Biological applications of quantum dots. Biomaterials. 2007; 28: 4717-32.
14. Ben-Ari ET. Nanoscale quantum dots hold promise for cancer applications. J Natl Cancer Inst. 2003; 95: 502-4.
15. Yong K-T, Hu R, Roy I, Ding H, Vathy LA, Bergey EJ, et al. Tumor targeting and imaging in live animals with functionalized semiconductor quantum rods. ACS Appl Mater Interfaces. 2009; 1: 710-9.
16. Qian HF, Dong CQ, Weng JF, Ren J. Facile one-pot synthesis of luminescent, water-soluble, and biocompatible glutathione-coated CdTe nanocrystals. Small. 2006; 2: 747-751.
17. Yong K-T, Law W-C, Roy I, Jing Z, Huang H, Swihart MT, et al. Aqueous phase synthesis of CdTe quantum dots for biophotonics. J Biophotonics, 2011; 4**:** 9-20.
18. Weissleder R, Kelly K, Sun EY, Shtatland T, Josephson L. Cell-specific targeting of nanoparticles by multivalent attachment of small molecules. Nat Biotechnol. 2005; 23: 1418-23.
19. Hezinger AFE, Tebear J, Goiferich A. Polymer coating of quantum dots - a powerful tool toward diagnostics and sensorics. Eur J Pharm Biopharm. 2008; 68: 138-52.
20. Law W-C, Yong K-T, Roy I, Xu G, Ding H, Bergey EJ, et al. Optically and magnetically doped organically modified silica nanoparticles as efficient magnetically guided biomarkers for two-photon imaging of live cancer cells. J Phys Chem C. 2008; 112: 7972-7.
21. Liu L, Law W-C, Yong K-T, Roy I, Ding H, Erogbogbo F, et al. Multimodal imaging probes based on Gd-DOTA conjugated quantum dot nanomicelles. Analyst. 2011; 136: 1881-6.
22. Erogbogbo F, Yong K-T, Roy I, Xu G, Prasad PN, Swihart MT. Biocompatible luminescent silicon quantum dots for imaging of cancer cells. ACS Nano.2008;2:873-8.
23. Jiang W, Papa E, Fischer H, Mardyani S, Chan WCW. Semiconductor quantum dots as contrast agents for whole animal imaging. Trends Biotechnol. 2004; 22: 607-9.
24. Bruchez M, Moronne M, Gin P, Weiss S, Alivisatos AP. Semiconductor Nanocrystals as Fluorescent Biological Labels. Science. 1998; 281: 2013-6.
25. Wu X, Liu H, Liu J, Haley KN, Treadway JA, Larson JP, et al. Immunofluorescent labeling of cancer marker Her2 and other cellular targets with semiconductor quantum dots. Nat Biotechnol. 2003; 21: 41-6.
26. Kabanov AV, Vinogradov SV, Suzdaltseva YG, Alakhov VY. Water-soluble block polycations as carriers for oligonucleotide delivery. Bioconjug Chem. 1995;6:639-43.
27. Kirchner C, Liedl T, Kudera S, Pellegrino T, Munoz Javier A, Gaub HE, et al. Cytotoxicity of colloidal CdSe and CdSe/ZnS nanoparticles. Nano Lett. 2004;5:331-8.
28. Kwon GS. Polymeric micelles for delivery of poorly water-soluble compounds. Crit Rev Ther Drug Carrier Syst. 2003; 20: 9.
29. Savic R, Luo L, Eisenberg A, Maysinger D. Micellar Nanocontainers distribute to defined cytoplasmic organelles. Science. 2003; 300: 615-8.
30. Torchilin VP, Lukyanov AN, Gao Z, Papahadjopoulos-Sternberg B. Immunomicelles: Targeted pharmaceutical carriers for poorly soluble drugs. Proc Natl Acad Sci USA. 2003; 100: 6039-44.
31. Trentin D, Hubbell J, Hall H. Non-viral gene delivery for local and controlled DNA release. J Control Release. 2005; 102: 263-75.
32. Missirlis D, Tirelli N, Hubbell JA. Amphiphilic hydrogel nanoparticles. Preparation, characterization, and preliminary assessment as new colloidal drug carriers. Langmuir. 2005; 21: 2605-13.
33. Kabanov AV, Batrakova EV. New technologies for drug delivery across the blood brain barrier. Curr Pharm Des. 2004; 10: 1355-63.
34. Salem AK, Searson PC, Leong KW. Multifunctional nanorods for gene delivery. Nat Mater. 2003; 2: 668-71.
35. Croy SR, Kwon GS. Polymeric micelles for drug delivery. Curr Pharm Des. 2006; 12: 4669-84.
36. Nayak S, Lyon LA. Soft Nanotechnology with soft nanoparticles. Angew Chem Int Ed Engl. 2005; 44: 7686-708.
37. Escorcia FE, McDevitt MR, Villa CH, Scheinberg DA. Targeted nanomaterials for radiotherapy. Nanomedicine. 2007; 2: 805-15.
38. Hall JB, Dobrovolskaia MA, Patri AK, McNeil SE. Characterization of nanoparticles for therapeutics. Nanomedicine. 2007; 2: 789-803.
39. Low PS, Henne WA, Doorneweerd DD. Discovery and development of folic-acid-based receptor targeting for imaging and therapy of cancer and inflammatory diseases. Acc Chem Res. 2007; 41: 120-9.
40. Pan D, Turner JL, Wooley KL. Folic acid-conjugated nanostructured materials designed for cancer cell targeting. Chem Commun. 2003;: 2400-1.
41. Geszke M, Murias M, Balan L, Medjahdi G, Korczynski J, Moritz M, et al. Folic acid-conjugated core/shell ZnS:Mn/ZnS quantum dots as targeted probes for two photon fluorescence imaging of cancer cells. Acta Biomater. 2011; 7: 1327-38.
42. Jian Y, et al. Folate-conjugated polymer micelles for active targeting to cancer cells: preparation, in vitro evaluation of targeting ability and cytotoxicity. Nanotechnology. 2008; 19: 045102.
43. Huang P, Xu C, Lin J, Wang C, Wang XS, Zhang CL, et al. Folic acid-conjugated graphene oxide loaded with photosensitizers for targeting photodynamic therapy. Theranostics. 2011;1:240-250.
44. Lu Y, Sega E, Leamon CP, Low PS. Folate receptor-targeted immunotherapy of cancer: mechanism and therapeutic potential. Adv Drug Deliv Rev. 2004; 56: 1161-76.
45. Ding H, Yong K-T, Law W-C, Roy I, Hu R, Wu F, et al. Non-invasive tumor detection in small animals using novel functional Pluronic nanomicelles conjugated with anti-mesothelin antibody. Nanoscale. 2011; 3: 1813-22.
46. Hsu YC, Chang YH, Yang CM. Swelling-agent-free synthesis of siliceous and functional mesocellular foam-like mesophases by using a carboxy-terminated triblock copolymer. Adv Funct Mater. 2008;18:1799-1808.
47. Bali D, King L, Kim S. Syntheses of new gramicidin A derivatives. Aust J chem. 2003;4:293-300.
48. Gaponik N, Talapin DV, Rogach AL, Eychmoller A, Weller H. Efficient phase transfer of luminescent thiol-capped nanocrystals: from water to nonpolar organic solvents. Nano Lett. 2002; 2: 803-6.
49. Tsay JM, Pflughoefft M, Bentolila LA, Weiss S. Hybrid approach to the synthesis of highly luminescent CdTe/ZnS and CdHgTe/ZnS nanocrystals. J Am Chem Soc. 2004; 126: 1926-7.